A chain of magnetic flux ropes in the magnetotail of Mars

J. P. Eastwood,[1] J. J. H. Videira,[1] D. A. Brain,[2] and J. S. Halekas[3]

Received 23 November 2011; revised 6 January 2012; accepted 6 January 2012; published 7 February 2012.

[1] The interaction of Mars with the solar wind leads to the formation of a magnetotail through which significant quantities of planetary plasma are transported. Of particular interest is the extent to which this plasma transport could be affected by magnetotail dynamics, for example by magnetic reconnection and flux rope formation. Here we show observations from Mars Global Surveyor of multiple flux ropes observed in Mars' magnetotail current sheet. A chain of at least three flux ropes is observed; based on the geometry of the encounter, the flux ropes are all being ejected in the same direction from a single dominant site and modeling shows that at least two of the flux ropes are close to being in a force free condition. Given geometrical considerations, it is likely that the flux ropes are generated sequentially rather than simultaneously, suggesting periodic generation via secondary instabilities at the reconnection site. **Citation:** Eastwood, J. P., J. J. H. Videira, D. A. Brain, and J. S. Halekas (2012), A chain of magnetic flux ropes in the magnetotail of Mars, *Geophys. Res. Lett.*, *39*, L03104, doi:10.1029/2011GL050444.

1. Introduction

[2] The interaction of Mars with the solar wind leads to the formation of an induced magnetotail [*Yeroshenko et al.*, 1990; *Nagy et al.*, 2004]. The magnetotail is a region through which there is significant escape of ionospheric material [*Lundin et al.*, 2008], and so it is important to ascertain the extent to which magnetotail dynamics may inhibit or enhance the transport of planetary plasma away from Mars. In particular, within the magnetotail is found the magnetotail current sheet, separating the two hemispheres of draped solar wind magnetic field [*Halekas et al.*, 2006]. The interaction between crustal fields and the draped field can lead to the formation and detachment of large magnetic flux ropes enabling the bulk removal of material [*Harnett*, 2009; *Brain et al.*, 2010; *Morgan et al.*, 2011]. It has been noted that at comets, bulk removal could also occur via disconnection across the tail current sheet [*Russell et al.*, 1986], analogous to the removal of plasma in the Earth's magnetotail via the formation of a Near-Earth Neutral Line [*Baker et al.*, 1996].

[3] Both processes rely on magnetic reconnection to reconfigure the topology of the plasma, but the strong normal magnetic field that typically results from the field draping has been thought to stabilize the induced magnetotail current sheet against reconnection [e.g., *Slavin et al.*, 1989]. However, evidence for this process occurring at Mars in the magnetotail current sheet has been presented [*Eastwood et al.*, 2008; *Halekas et al.*, 2009]. Thus far this evidence is derived from observations of the ion diffusion region, where the ions decouple from the magnetic field leading to the formation of Hall magnetic fields that can be identified in data. This region is relatively small, and so observations are rare since the spacecraft made in situ measurements [*Halekas et al.*, 2009].

[4] In order to better understand the role that reconnection and flux ropes may play transporting plasma at Mars, a key issue is to understand their dynamics, including whether multiple flux ropes can be produced in a single event, since this might change considerations of plasma transport efficiency. Simulations show that multiple flux ropes can be produced via secondary instabilities during reconnection [*Drake et al.*, 2006; *Karimabadi et al.*, 2007]. Alternatively, multiple flux ropes can also be formed if the onset of reconnection occurs at several points simultaneously [*Schindler*, 1974; *Slavin et al.*, 2003; *Eastwood et al.*, 2005].

[5] Here we present the first observations of a chain of flux ropes in Mars's magnetotail, using observations from the Mars Global Surveyor (MGS) magnetometer/electron reflectometer (MAG/ER) experiment [*Acuña et al.*, 1998]. This new data shows that multiple flux ropes, rather than a single flux rope, can in fact be generated in a single event. This must be accounted for in future studies attempting to model the Mars – solar wind interaction and to understand the transport of plasma through Mars' magnetotail by bulk escape mechanisms.

2. Overview

[6] An overview of the observations, made on 14 January 2000 when MGS was in its 400 km 2 am/2 pm mapping orbit, are shown in Figures 1a–1d; two hours of data (~1.5 orbits) are shown. The bar below Figure 1d indicates whether the spacecraft was illuminated (black = nightside). Figures 1a and 1b show the electron energy flux and the 120 eV electron pitch angle distribution (PAD) at 24 s resolution (ER observes a 14° × 360° strip of sky; if **B** does not lie in the plane of the detector, only a partial PAD can be constructed). Figures 1c and 1d show |B| and **B** at 1.5 s resolution in MSO coordinates ($\mathbf{X_{MSO}}$ points sunward, $\mathbf{Y_{MSO}}$ lies in the ecliptic and points opposite to the direction of orbital motion, and $\mathbf{Z_{MSO}}$ is perpendicular to the ecliptic). The sections of the |B| time series colored red are regions where crustal fields are thought to be present, based on existing models [*Cain et al.*, 2003]. Between 14:45UT–14:55UT, B_x reverses in sign, indicating a magnetotail current sheet crossing [*Halekas et al.*, 2006].

[7] The current sheet crossing is shown in more detail in Figures 1e–1i. It can be seen that there is not a smooth simple transition from one side of the current sheet to the

[1]Blackett Laboratory, Imperial College London, London, UK.
[2]LASP, University of Colorado at Boulder, Boulder, Colorado, USA.
[3]Space Sciences Laboratory, University of California, Berkeley, California, USA.

0094-8276/12/2011GL050444

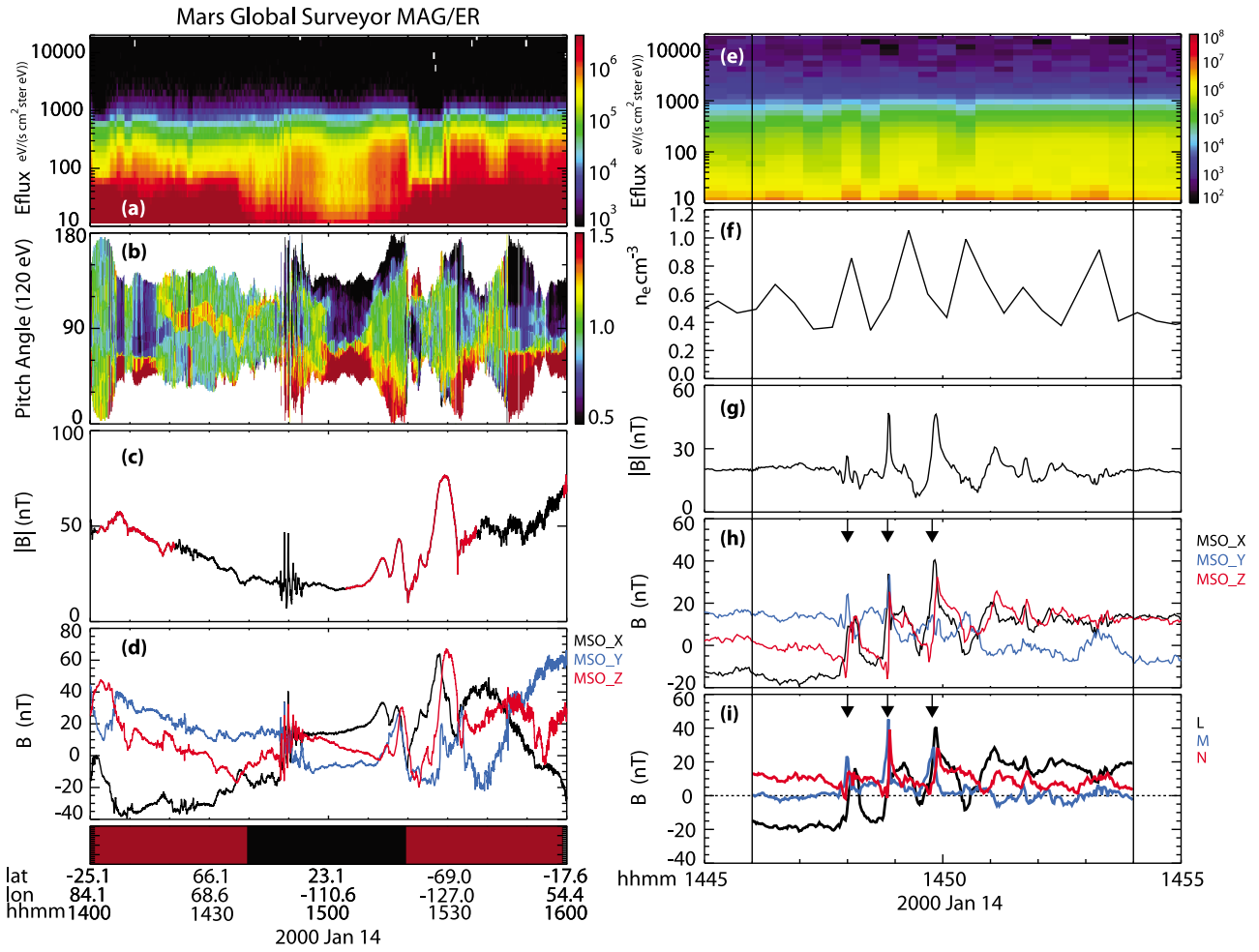

Figure 1. Overview of the MGS data. (a) Electron energy flux, (b) pitch angle distribution at 120 eV, (c) magnetic field strength; red indicates regions of crustal fields, (d) magnetic field components in MSO coordinates. The bottom color bar indicates where MGS was illuminated, and thus dayside (red) and nightside (black). The x-axis labels indicate the latitude and longitude of MGS. Zoom in showing the MGS data between 14:45UT and 14:55UT. (e) Electron energy flux, (f) electron density estimate, (g) magnetic field strength, (h) magnetic field components in MSO coordinates, (i) magnetic field components in minimum variance coordinates.

other. The electron density, calculated by applying a Maxwellian fit to the electron distribution assuming isotropy, shows that n_e is anti-correlated with |B|. Figure 1i shows the magnetic field transformed into a local coordinate system based on a minimum variance analysis (MVA) of the magnetic field observed between 14:46UT–14:54UT [*Sonnerup and Scheible*, 1998]. **L** (maximum variance direction)-**M** (intermediate)-**N** (minimum) is a right handed triple where **N** is the current sheet normal and **L** contains the main magnetic field reversal; **L** = [0.783, −0.381, 0.492], **M** = [0.611, 0.622, −0.490] and **N** = [−0.120, 0.684, 0.719]. The current sheet normal **N** is northward ($\mathbf{N}_z > 0$), and so points opposite to the direction of spacecraft motion.

[8] Referring to Figure 1i, it can be seen that overall, B_L reverses sign from negative to positive values. The magnetic field normal to the current sheet B_N is on average positive ($\langle B_N \rangle \sim 10$ nT), and relatively constant. There are at least three distinct bi-polar oscillations in the B_N component of the magnetic field (at 14:48:00UT, 14:48:50UT, 14:49:50UT, marked with arrows), correlated with enhancements in both |B| and B_M. These structures are thus qualitatively consistent with being flux ropes [*Elphic et al.*, 1986; *Slavin et al.*, 2003; *Briggs et al.*, 2011].

3. Flux Rope Properties

[9] In order to determine more quantitatively the properties of these structures, we fit the data to a force-free flux rope model [*Burlaga*, 1988; *Lepping et al.*, 1990]. Under force-free conditions, and assuming that magnetic forces dominate, $\mathbf{J} \times \mathbf{B} = \mathbf{0}$. A solution of this equation is a cylindrically symmetric helical magnetic field: $B_z(r) = B_0 J_0(\alpha r)$, $B_\theta(r) = B_0 H J_1(\alpha r)$, $B_r = 0$, where B_0 is the peak core magnetic field, α is constant and H is the handedness [*Burlaga*, 1988, and references therein].

[10] To fit the data to the model, it is assumed that the spacecraft follows a straight-line trajectory through the rope. This trajectory is defined by its impact factor i.e. the closest approach to the flux rope axis. The interval of interest is first transformed using MVA and the intermediate variance direction is identified as the axis of the flux rope [e.g., *Lepping et al.*, 1990]. A least squares fit is then performed

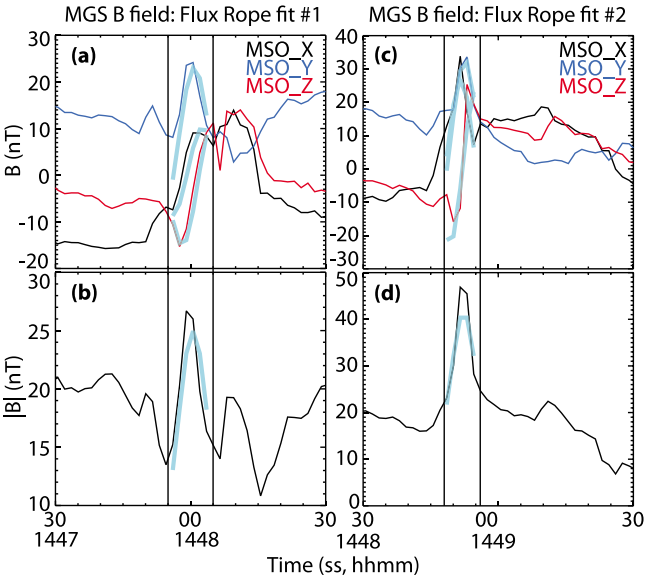

Figure 2. Flux rope fitting. (a, b) Fit to the first flux rope at 14:48:00UT. (c, d) Fit to the second flux rope at 14:48:50UT. Data is shown in MSO coordinates and the model field variation is overlaid in cyan.

between the data and the model, varying the model core field and the model impact parameter.

[11] For the first flux rope, observed between 14:47:55UT–14:48:05UT, the axis orientation derived from the MVA analysis is (0.374, 0.841, −0.391). The eigenvalues are well separated ($\{\lambda_1, \lambda_2, \lambda_3\} = \{107.4, 49.7, 0.88\}$), lending confidence to this identification.

[12] The least squares fit to the model leads to an axial field strength $B_0 = 25.4$ nT, $\alpha = 0.8$ and a closest approach parameter $y_0 = 0.15$ (where 0 indicates the centre of the flux rope and 1 indicates where the magnetic field in the model is perpendicular to the axis). The model magnetic field is shown overlaid on the observed data in Figures 2a and 2b; there is a good agreement between the model and the data.

[13] The same procedure was applied to the second flux rope, observed between 14:48:48UT–14:48:56UT. In this case, the axis orientation was found to be (0.742, 0.657, 0.135), with eigenvalues $\{\lambda_1, \lambda_2, \lambda_3\} = \{319.9, 95.4, 1.51\}$. The best-fit model corresponds to an axial field strength $B_0 = 42.2$ nT, $\alpha = 0.96$ and impact parameter $y_0 = 0.15$. Figures 2c and 2d shows the data together with the best-fit model. Again there is good agreement between the model and the data. The third flux rope occurred between 14:49:45UT–14:49:55UT. However, a good fit was not recovered. In particular, the impact parameter $y_0 = 0.45$, which may indicate that it is not appropriate to use MVA to identify the flux rope axis, since the spacecraft apparently passed too far from the center of the flux rope [*Rees*, 2002]. We also note that MVA would not necessarily work if the structure were not force free [*Xiao et al.*, 2004].

4. Discussion

[14] Although the very good agreement between the force-free model and the data (in the first two cases) lends confidence to the flux rope interpretation, further tests for consistency can be made. Geometrically, if produced by reconnection, the flux rope axes ought to be perpendicular to the current sheet normal and aligned with the current sheet **M** axis, although dynamic effects (e.g., variable reconnection rate across the X-line or differential plasma flow) could cause this to change. The alignment angle of the flux rope axis to the current sheet **M** axis is 19° and 37° respectively for the first and second flux ropes, and so the flux ropes are indeed appropriately aligned relative to the overall magnetotail configuration. Figure 3 shows a sketch describing the geometry of the encounter. MGS moves in the $-\mathbf{N}$ direction (i.e., towards the south pole in the $-Z_{MSO}$ direction) from $B_L < 0$ to $B_L > 0$. Since $\langle B_N \rangle$ is positive, we can thus determine the overall field geometry. The curvature of the field is consistent with MGS being on the anti-sunward side (i.e. in the direction of decreasing **L**) of an X-line, whose presence is necessary to create the moving flux rope chain as described in the introduction.

[15] Based on the overall magnetic field geometry, we can independently verify their signature in the spacecraft data. The flux ropes are observed when MGS is located in the current sheet. The spacecraft velocity is of the order of a few km s^{-1}, and this is substantially less than the characteristic flow speed with which the flux ropes are likely to convect downtail [*Harnett*, 2009]. As such MGS is effectively stationary in the current sheet as the flux ropes pass over (even with possible current sheet flapping). This means that there should be a negative/positive perturbation in B_N. Each observed negative/positive perturbation in B_N is thus consistent with a flux rope moving in the **-L** direction.

[16] We note that the current sheet is rather thick, as indicated by the relatively large mean B_N, and so it is of interest to understand why it is unstable to reconnection and flux rope production. In particular this may suggest that in the region where the flux ropes initially formed, the current sheet was significantly thinner. Figure 1d indicates that shortly after observing the flux ropes, MGS travelled through a significant crustal field region on the dayside near the terminator. It has recently been shown that flux ropes are produced from near these crustal field regions [*Brain et al.*, 2010; *Morgan et al.*, 2011], and so these flux ropes may also be associated with

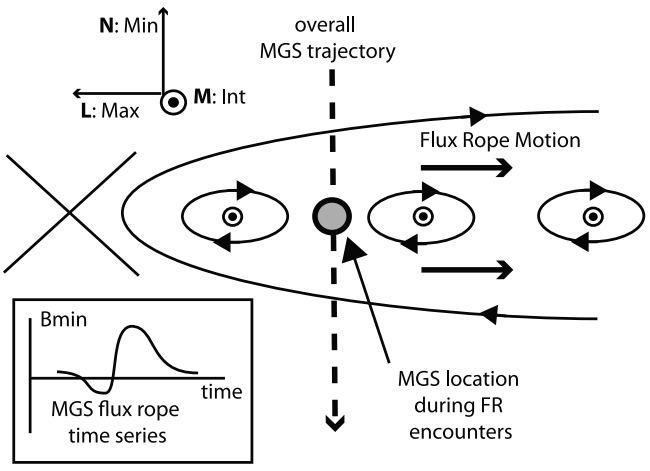

Figure 3. Cartoon showing the relative orientation of the MGS orbit and the current sheet. Whilst in the center of the current sheet, MGS observed three distinct flux ropes, corresponding to the negative/positive variation in B_N. This is consistent with the overall geometry of the current sheet.

this region, where the interaction of the draped field and the crustal fields could lead to thin current sheet formation. Each flux rope lasts approximately 10 seconds, and if they convect downtail at 40 kms^{-1} [*Harnett*, 2009], then their size is comparable to the altitude of MGS. This implies that they are actually convecting from around the side of the planet, rather than being generated in the magnetotail. This may also suggest that the flux ropes are produced sequentially from a single region rather than being produced in a multiple X-line scenario, since the system size is insufficient to simultaneously contain several widely-spaced X-lines; this is consistent with recent simulations showing the sequential production of flux ropes [*Harnett*, 2009], but further dedicated simulations and modelling of this event is necessary.

5. Conclusions

[17] The data strongly suggest that MGS encountered a chain of tailward moving flux ropes on the nightside of Mars. Such flux ropes are entrained in plasma flows generated by a dominant X-line. Unfortunately, this cannot be measured by MGS, but the analysis of the available data is entirely consistent with this scenario. Based on considerations of geometry, it seems more likely that these flux ropes are being generated sequentially at a single site rather than by the simultaneous formation of multiple X-lines. Although observations of this type are quite rare in MGS data, this event is not unique; in a database of 1116 MGS magnetotail current sheet crossings [*Halekas et al.*, 2006], we have identified 45 examples where multiple flux ropes were observed, however the event presented here is the cleanest example.

[18] A major limitation of existing Mars datasets is the lack of simultaneous measurements of the magnetic field and the thermal plasma, which also precludes an analysis of the effects of heavy ions on flux rope formation. Here, the absence of plasma velocity measurements means that although it can be shown that the magnetic field structure is consistent with a chain of flux ropes, it is not possible to scale the time series data and determine the absolute size of the flux ropes, and thus important physical parameters such as volume and plasma content. Future data will be crucial in elucidating the exact nature of Mars' magnetotail dynamics, and it is expected that the next generation of spacecraft studying the Mars solar wind interaction will observe similar multiple flux rope events.

[19] **Acknowledgments.** JPE is supported by an STFC Advanced Fellowship at ICL and the work of JJHV was performed under the auspices of the Undergraduate Research Opportunity Programme at ICL. This work was supported by NASA grant NNX08AK95G.

[20] The Editor thanks James Slavin and David Sibeck for their assistance in evaluating this paper.

References

Acuña, M. H., et al. (1998), Magnetic field and plasma observations at Mars: Initial results of the Mars Global Surveyor mission, *Science*, *279*, 1676–1680, doi:10.1126/science.279.5357.1676.

Baker, D. N., T. I. Pulkkinen, V. Angelopoulos, W. Baumjohann, and R. L. McPherron (1996), Neutral line model of substorms: Past results and present view, *J. Geophys. Res.*, *101*, 12,975–13,010, doi:10.1029/95JA03753.

Brain, D. A., A. H. Baker, J. Briggs, J. P. Eastwood, J. S. Halekas, and T.-D. Phan (2010), Episodic detachment of Martian crustal magnetic fields leading to atmospheric plasma escape, *Geophys. Res. Lett.*, *37*, L14108, doi:10.1029/2010GL043916.

Briggs, J. A., D. A. Brain, M. L. Cartwright, J. P. Eastwood, and J. S. Halekas (2011), A statistical study of flux ropes in the Martian magnetosphere, *Planet. Space Sci.*, *59*, 1498–1505, doi:10.1016/j.pss.2011.06.010.

Burlaga, L. F. (1988), Magnetic clouds and force-free fields with constant alpha, *J. Geophys. Res.*, *93*, 7217–7224, doi:10.1029/JA093iA07p07217.

Cain, J. C., B. B. Ferguson, and D. Mozzoni (2003), An n = 90 internal potential function of the Martian crustal magnetic field, *J. Geophys. Res.*, *108*(E2), 5008, doi:10.1029/2000JE001487.

Drake, J. F., M. Swisdak, K. M. Schoeffler, B. N. Rogers, and S. Kobayashi (2006), Formation of secondary islands during magnetic reconnection, *Geophys. Res. Lett.*, *33*, L13105, doi:10.1029/2006GL025957.

Eastwood, J. P., D. G. Sibeck, J. A. Slavin, M. L. Goldstein, B. Lavraud, M. Sitnov, S. Imber, A. Balogh, E. A. Lucek, and I. Dandouras (2005), Observations of multiple X-line structure in the Earth's magnetotail current sheet: A Cluster case study, *Geophys. Res. Lett.*, *32*, L11105, doi:10.1029/2005GL022509.

Eastwood, J. P., D. A. Brain, J. S. Halekas, J. F. Drake, T. Phan, M. Oieroset, D. G. Mitchell, R. P. Lin, and M. H. Acuña (2008), Evidence for collisionless reconnection at Mars, *Geophys. Res. Lett.*, *35*, L02106, doi:10.1029/2007GL032289.

Elphic, R. C., C. A. Cattell, K. Takahashi, S. J. Bame, and C. T. Russell (1986), ISEE-1 and 2 observations of magnetic flux ropes in the magnetotail: FTE's in the plasma sheet?, *Geophys. Res. Lett.*, *13*, 648–651, doi:10.1029/GL013i007p00648.

Halekas, J. S., D. A. Brain, R. J. Lillis, M. O. Fillingim, D. L. Mitchell, and R. P. Lin (2006), Current sheets at low altitudes in the Martian magnetotail, *Geophys. Res. Lett.*, *33*, L13101, doi:10.1029/2006GL026229.

Halekas, J. S., J. P. Eastwood, D. A. Brain, T.-D. Phan, M. Øieroset, and R. P. Lin (2009), In situ observations of reconnection Hall magnetic fields at Mars: Evidence for ion diffusion region encounters, *J. Geophys. Res.*, *114*, A11204, doi:10.1029/2009JA014544.

Harnett, E. M. (2009), High-resolution multifluid simulations of flux ropes in the Martian magnetosphere, *J. Geophys. Res.*, *114*, A01208, doi:10.1029/2008JA013648.

Karimabadi, H., W. Daughton, and J. Scudder (2007), Multi-scale structure of the electron diffusion region, *Geophys. Res. Lett.*, *34*, L13104, doi:10.1029/2007GL030306.

Lepping, R. P., J. A. Jones, and L. F. Burlaga (1990), Magnetic field structure of interplanetary magnetic clouds at 1 AU, *J. Geophys. Res.*, *95*, 11,957–11,965, doi:10.1029/JA095iA08p11957.

Lundin, R., S. Barabash, M. Holmström, H. Nilsson, M. Yamauchi, M. Fraenz, and E. Dubinin (2008), A comet-like escape of ionospheric plasma from Mars, *Geophys. Res. Lett.*, *35*, L18203, doi:10.1029/2008GL034811.

Morgan, D. D., D. A. Gurnett, F. Akalin, D. A. Brain, J. S. Leisner, F. Duru, R. A. Frahm, and J. D. Winningham (2011), Dual-spacecraft observation of large-scale magnetic flux ropes in the Martian ionosphere, *J. Geophys. Res.*, *116*, A02319, doi:10.1029/2010JA016134.

Nagy, A. F., et al. (2004), The plasma environment of Mars, *Space Sci. Rev.*, *111*, 33–114, doi:10.1023/B:SPAC.0000032718.47512.92.

Rees, A. (2002), Ulysses observations of magnetic clouds in the 3-D heliosphere, PhD thesis, Imp. Coll. of Sci. Technol. and Med., Univ. of London, London.

Russell, C. T., M. A. Saunders, J. L. Phillips, and J. A. Fedder (1986), Near-tail reconnection as the cause of cometary tail disconnections, *J. Geophys. Res.*, *91*, 1417–1423, doi:10.1029/JA091iA02p01417.

Schindler, K. (1974), A theory of the substorm mechanism, *J. Geophys. Res.*, *79*, 2803–2810, doi:10.1029/JA079i019p02803.

Slavin, J. A., D. S. Intriligator, and E. J. Smith (1989), Pioneer Venus Orbiter magnetic field and plasma observations in the Venus magnetotail, *J. Geophys. Res.*, *94*, 2383–2398, doi:10.1029/JA094iA03p02383.

Slavin, J. A., R. P. Lepping, J. Gjerloev, D. H. Fairfield, M. Hesse, C. J. Owen, M. B. Moldwin, T. Nagai, A. Ieda, and T. Mukai (2003), Geotail observations of magnetic flux ropes in the plasma sheet, *J. Geophys. Res.*, *108*(A1), 1015, doi:10.1029/2002JA009557.

Sonnerup, B. U. Ö., and M. Scheible (1998), Minimum and maximum variance analysis, in *Analysis Methods for Multi-Spacecraft Data*, edited by G. Paschmann and P. W. Daly, pp. 185–220, Int. Space Sci. Inst., Bern.

Xiao, C. J., Z. Y. Pu, Z. W. Ma, S. Y. Fu, Z. Y. Huang, and Q. G. Zong (2004), Inferring of flux rope orientation with the minimum variance analysis technique, *J. Geophys. Res.*, *109*, A11218, doi:10.1029/2004JA010594.

Yeroshenko, Y., W. Riedler, K. Schwingenschuh, J. G. Luhmann, M. Ong, and C. T. Russell (1990), The magnetotail of Mars: Phobos observations, *Geophys. Res. Lett.*, *17*, 885–889, doi:10.1029/GL017i006p00885.

D. A. Brain, LASP, University of Colorado at Boulder, 1234 Innovation Dr., Boulder, CO 80303, USA.

J. P. Eastwood and J. J. H. Videira, Blackett Laboratory, Imperial College London, Prince Consort Road, London SW7 2AZ, UK. (jonathan.eastwood@imperial.ac.uk)

J. S. Halekas, Space Sciences Laboratory, University of California, 7 Gauss Way, Berkeley, CA 94720, USA.